Gravity-induced liquid crystal phase transitions of colloidal platelets

David van der Beek
Van't Hoff Laboratory for Physical and Colloid Chemistry, Utrecht University, Padualaan 8, 3584 CH Utrecht, The Netherlands

Tanja Schilling
Institut für Physik, Johannes Gutenberg Universität, 55099 Mainz, Germany

Henk N. W. Lekkerkerker
Van't Hoff Laboratory for Physical and Colloid Chemistry, Utrecht University, Padualaan 8, 3584 CH Utrecht, The Netherlands

(Received 4 May 2004; accepted 24 June 2004)

The influence of gravity on a suspension of sterically stabilized colloidal gibbsite platelets is studied. An initially isotropic-nematic biphasic sample of such a suspension develops a columnar phase on the bottom on prolonged standing. This phenomenon is described using a simple osmotic compression model. We performed Monte Carlo simulations of cut spheres with aspect ratio $L/D = 1/15$ and took data from the literature to supply the equations of state required for the model. We find that the model describes the observed three-phase equilibrium quite well. © *2004 American Institute of Physics.* [DOI: 10.1063/1.1783231]

I. INTRODUCTION

The influence of gravitational compression on suspensions of colloidal particles has received attention for a long time. At the beginning of the previous century Jean Perrin[1,2] verified with simple yet brilliant experiments that the concentration of colloidal particles in dilute suspension varied exponentially with height when allowed to reach dynamic equilibrium in the earth's gravitational field. From these measurements he obtained Avogadro's number. The extension of the ideas of Perrin to interacting systems has also appeared to be very fruitful.[3–6] Crandall and Williams[7] measured the effect of the earth's gravitational field on the lattice constant of a colloidal crystal of polystyrene spheres. Perhaps even more interesting is the effect of gravity on multiple phases. Takano and Hachisu[8] pioneered the measurement of the coexistence pressure of the disorder-order transition in a sedimented dispersion of monodisperse latex particles. At an electrolyte concentration of 10 mM they found good agreement with results of computer simulations for hard spheres.[9] Hachisu and Takano[10] and later Piazza, Bellini, and Degiorgio[11] and Rutgers and co-workers[12] explored the possibility to obtain the equation of state both in the fluid as well as the crystal state from the concentration profile as a function of height. In all three cases good agreement with the hard-sphere equation of state was obtained at sufficiently high salt concentration. The equivalent of this in computer simulations was done by Biben, Hansen, and Barrat.[13]

For anisotropic particles, i.e., rods and plates, experiments are much more limited. Colloidal hard rods and plates show intrinsically richer phase behavior than hard spheres due to their shape. Apart form the isotropic fluid (I) and crystal phase, the nematic (N), smectic and columnar (C) phases are encountered, so when the effect of gravity is also taken into account, this allows for the simultaneous coexistence of more than two phases. Only a few observations are available. In the 1950s, Oster[14] reported on an I-N biphasic suspension of tobacco mosaic virus rods that developed a third (Smectic-A) phase on the bottom of the sample after some time, an observation that was later confirmed by Kreibig and Wetter.[15] In neither case, a quantitative analysis was performed. Brian, Frisch, and Lerman[16] investigated sedimented suspensions of DNA-fragments at high salt concentration and analyzed their results in terms of a scaled particle theory equation of state.

Very recently, a model system of hard plates was developed in our laboratory, consisting of sterically stabilized gibbsite platelets dispersed in toluene.[17] This suspension showed the liquid crystal phase transitions predicted for such particles,[18,19] i.e., isotropic to nematic[17] and nematic to columnar.[20] On prolonged standing we find that an initially biphasic I-N sample developed a third phase on the bottom that we identify as a columnar phase on the basis of the optical Bragg reflections. This phenomenon can be explained by a simple osmotic compression model.[21,22] Using equations of state obtained from literature and from Monte Carlo computer simulations that we performed, we find good agreement with the experimentally determined individual phase heights.

II. EXPERIMENTAL SECTION

We synthesized a colloidal suspension of sterically stabilized gibbsite [$Al(OH)_3$] platelets according to van der Kooij and Lekkerkerker.[17] Transmission electron microscopy (TEM) and atomic force microscopy were used to determine the average diameter and thickness of the particle core, thus disregarding the steric stabilizer. We found $\langle D \rangle = 230$ nm and $\langle L \rangle = 13$ nm and a polydispersity of about 22% in both dimensions. The thickness of the sterically stabilizing polyisobutene brush is estimated at 2–3 nm, where we take into

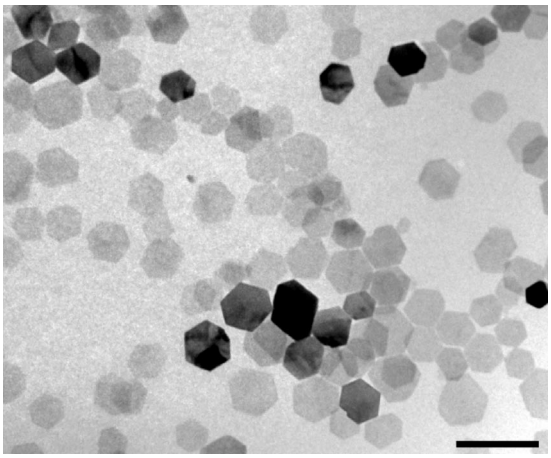

FIG. 1. Transmission electron microscope graph showing the gibbsite platelets (the stabilizing polyisobutene layer is not visible). The hexagonal shape of the nanocrystals is easily observed. The scale bar denotes 500 nm.

account a certain maximum stretching length for the polymer at this specific molar weight and an estimate for the extent of the steric repulsion. This gives us effective dimensions of $D_{\mathrm{eff}}=235$ nm and $L_{\mathrm{eff}}=18$ nm and hence an aspect ratio of $L/D\approx 1/13$. Figure 1 shows a TEM micrograph of the platelets.

We investigated the phase behavior in the gravitational field by preparing a sample of this dispersion at a concentration in the *I*-*N* biphasic gap, in a glass cell with a height of about 30 mm. On a time scale of several days, the sample separated into an isotropic upper phase and a birefringent nematic lower phase. The phase-separated sample was investigated on a regular basis for one and a half year. After a few months, a third phase evolved on the bottom of the cell, which appeared to be a columnar phase, see Fig. 2. The columnar phase developed bright Bragg reflections (deep red to blue, depending on the angle of the incident light) in time. After one year, the sample did not show any appreciable change anymore and we found the heights of the phases to be 15.5, 8.5, and 2.5 mm for the isotropic, nematic, and columnar phase, respectively.

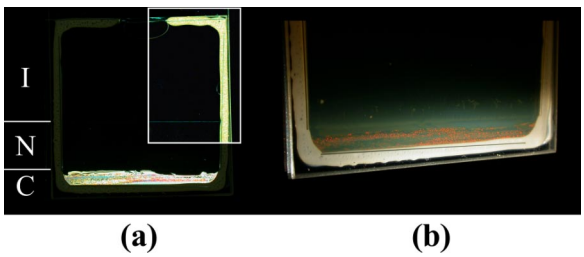

FIG. 2. (Color online) The three-phase sedimentation equilibrium. Photograph (a) depicts the complete sample between crossed polarizers, where the upper right part is digitally enhanced to visualize the *I*-*N* interface. The columnar phase contains a dark region at the upper right of the phase, probably due to orientation of the platelets along the sample walls. Although not clearly visible, the *N*-*C* interface is horizontal and sharp. (b) shows the columnar phase illuminated with white light to capture the red Bragg reflections.

III. MODEL

A. Sedimentation-diffusion equilibrium

Consider a suspension of monodisperse, hard disks with number density $n(z)$ and buoyant mass $m^*=v_p(\rho_p-\rho_0)$, with v_p the single particle volume and ρ_p and ρ_0 the mass densities of the particle and solvent, respectively. When sedimentation-diffusion equilibrium is reached, Eq. (1) describes the complete system:[21,22]

$$-\left(\frac{\partial\Pi}{\partial n}\right)\frac{\partial n}{\partial z}=m^*gn. \tag{1}$$

To simplify the approach, we define reduced quantities. The pressure will be given by $\tilde{\Pi}=\Pi D^3/k_BT$, the gravitational length scale $\xi=k_BT/m^*g$, and the reduced concentration $c=nD^3$. Substituting these expressions in Eq. (1) yields

$$\frac{1}{c}\left(\frac{\partial\tilde{\Pi}}{\partial c}\right)dc=-\frac{dz}{\xi}. \tag{2}$$

For a single phase, the height $H=z_{top}-z_{bottom}$ is found by integrating Eq. (2) from c_{top} to c_{bottom}

$$H=\int_{z_{bottom}}^{z_{top}}dz=-\xi\int_{c_{bottom}}^{c_{top}}\frac{1}{c}\frac{\partial\tilde{\Pi}}{\partial c}dc. \tag{3}$$

The average concentration $\overline{c}$ of this phase is given by

$$\overline{c}=\frac{\int_{c_{bottom}}^{c_{top}}c(z)dz}{\int_{z_{bottom}}^{z_{top}}dz}=\frac{1}{H}\int_{c_{bottom}}^{c_{top}}c(z)\frac{dz}{dc}dc. \tag{4}$$

Using Eq. (2) this yields

$$\overline{c}=-\frac{\xi}{H}\int_{c_{bottom}}^{c_{top}}\frac{\partial\tilde{\Pi}}{\partial c}dc=\frac{\xi}{H}[\tilde{\Pi}(c_{bottom})-\tilde{\Pi}(c_{top})]. \tag{5}$$

For multiple phases in sedimentation equilibrium, Eqs. (3) and (5) apply to each of the phases. The total sample height H^{sample} is obviously the sum of the individual phase heights H^{α}

$$H^{sample}=\sum_{\alpha}H^{\alpha}, \tag{6}$$

where the summation ranges over all the phases. The average overall sample concentration $\overline{c}^{sample}$ can now be written as

$$\overline{c}^{sample}=\frac{1}{H^{sample}}\sum_{\alpha}H^{\alpha}\overline{c}^{\alpha}=\frac{\xi}{H^{sample}}\sum_{\alpha}[\tilde{\Pi}(c^{\alpha}_{bottom})-\tilde{\Pi}(c^{\alpha}_{top})], \tag{7}$$

where the $\overline{c}^{\alpha}$ are the average phase concentrations. Taking into account that for two coexisting phases α and β (where α on top of β)

$$\tilde{\Pi}(c^{a}_{bottom})=\tilde{\Pi}(c^{\beta}_{top}), \tag{8}$$

Eq. (7) together with Eq. (5) leads to the surprisingly simple result

$$\overline{c}^{sample}=\frac{\xi}{H^{sample}}[\tilde{\Pi}(c^{sample}_{bottom})-\tilde{\Pi}(c^{sample}_{top})]. \tag{9}$$

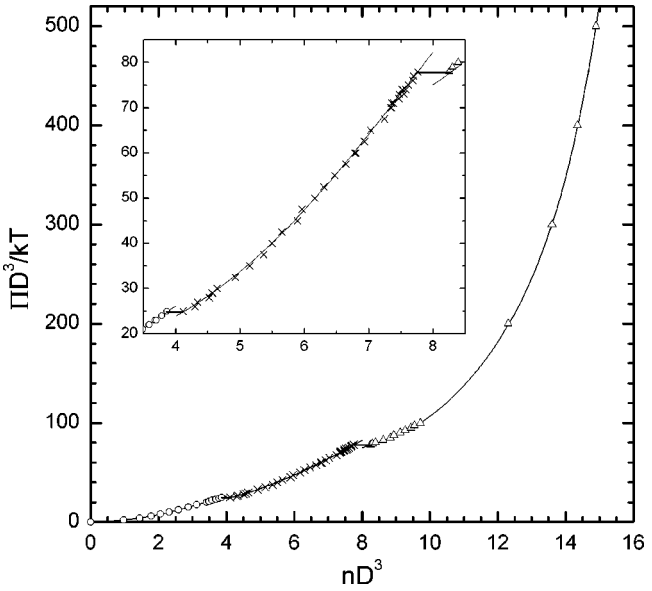

FIG. 3. The equation of state from MC simulations for cut spheres with aspect ratio $L/D=1/15$. Circles are for the isotropic, crosses for the nematic and triangles for the columnar phase. The phase transitions are indicated with thick lines. The inset shows the region of the phase transitions.

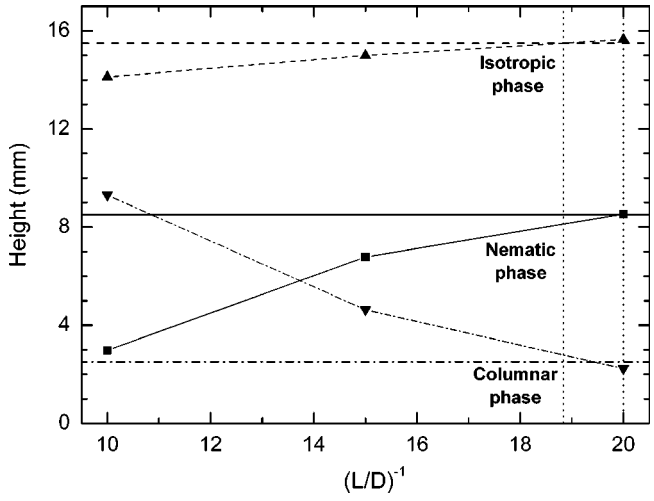

FIG. 4. The heights of the individual phases vs aspect ratio, using the values given in Table II. For each phase, the measured (horizontal lines) and calculated heights (lines with symbols) are given. Dashed lines refer to the isotropic, solid lines refer to the nematic, and dash-dotted lines refer to the columnar phase. The vertical dotted lines indicate the interval (around $L/D=1/19$) where our experiment is quite well described.

B. Equation of state

In order to calculate the individual phase heights for a given overall concentration from Eqs. (3) and (9) we need to know the equation of state for the various coexisting phases. Zhang, Reynolds, and van Duijneveldt[19] performed MC computer simulations on cut spheres (particles obtained by slicing two caps off a sphere of diameter D, at two planes parallel to the equatorial plane with equal distance L/2) with aspect ratios of $L/D=1/10$ and $L/D=1/20$ and obtained equations of state for both aspect ratios. As our particles have an aspect ratio that is in between these values, we decided to fill the gap ourselves.

We have performed constant-N-P-T Monte Carlo simulations of a system of 1000 cut spheres with aspect ratio $L/D=1/15$. The box was cubic with independently variable side lengths to accommodate the columnar phase. The equation of state shown in Fig. 3 was obtained by expansion from the columnar phase into the isotropic as well as compression from the isotropic to the columnar. For each pressure we equilibrated for 400 000 MC steps.

The equation of state shows two density jumps indicating first order phase transitions: the I-N transition and the N-C transition. Close to the transitions the system showed a small hysteresis in both cases. This is due to finite simulation time and finite system size—no fluctuation occurred on the time scale of the simulation that took the system over the nucleation barrier to the next phase. We could nevertheless locate the I-N transition to the accuracy we desired for this work, and found $c_I=3.86$ and $c_{NI}=4.11$, with a corresponding pressure of $\tilde{\Pi}_{I\text{-}N}=24.8\pm1.0$. The hysteresis around the N-C transition, however, was too strong. From the work of Zhang, Reynolds, and van Duijneveldt[19] it appears that the N-C phase transition concentrations (expressed as a volume fraction ϕ) are independent of the aspect ratio (either 1/10 or 1/20). Therefore, we interpolate to obtain the N-C transition concentrations in our system and find $c_{NC}=7.75$ and $c_C=8.29$ using the relation $\phi=(\pi/12)(L/D)[3-(L/D)^2]c$. The pressure at the transition is found to be $\tilde{\Pi}_{N\text{-}C}=77.8\pm1.0$. The resulting equation of state is plotted in Fig. 3. In order to use the obtained simulation data in our model, we fitted polynomials to the three branches of the equation of state. Thus, three sets parameters were obtained that are given in Table I.

IV. RESULTS AND DISCUSSION

We now turn to the analysis of the sedimentation equilibrium that we have observed. The key parameter in our system is the gravitational length scale ξ defined above. Taking into account that for our hexagonal particles $v_p=3/8\sqrt{3}D^2L=6.5\times10^{-22}$ m^3 and $\rho_p-\rho_0=835$ kg/m^3, we find $\xi=0.77$ mm. The measured total sample height is 26.4 mm, which yields a dimensionless height of $H/\xi=34.3$. By setting the overall concentration to a concentration in the I-N biphasic gap (as imposed by the experiment) we calculate the

TABLE I. The fitting parameters to our simulation data for the equation of state for cut spheres with $L/D=1/15$. The equation of state is given by $\tilde{\Pi}=\Sigma_{n=1}^{6}A_nc^n$, where $\tilde{\Pi}=\Pi D^3/k_BT$ and $c=nD^3$.

Phase	c	A_1	A_2	A_3	A_4	A_5	A_6
Isotropic	0–3.86	1	0.79432	0.44616	−0.07468	0	0
Nematic	4.11–7.75	11.8418	−4.1226	0.83763	−0.04333	0	0
Columnar	8.29–15.0	−321.03944	170.44185	−34.54128	3.43735	−0.16856	0.00329678

TABLE II. Heights in millimeters of the individual phases after settling of the sedimentation-diffusion equilibrium, as measured and calculated.

Phase	Measured height	Calculated height with $L/D=1/10$	Calculated height with $L/D=1/15$	Calculated height with $L/D=1/20$
I	15.5	14.1	15.0	15.7
N	8.5	3.0	6.8	8.5
C	2.5	9.3	4.6	2.2

individual phase heights using the model detailed in Sec. III A and the equations of state of Zhang, Reynolds, and van Duijneveldt[19] and the one we obtained. The results are presented in Table II and Fig. 4 visualizes the evolution of the calculated phase heights with aspect ratio. From this figure it is clear that at our experimental aspect ratio of 1/13 the phase heights are not correctly predicted. However, a fairly good description is obtained for $L/D=1/19$. A similar difference is found for a previous study on the same colloidal suspension of sterically stabilized gibbsite platelets. van der Kooij, Kassapidou, and Lekkerkerker[20] found the experimental aspect ratio to be 1/14 for their platelets. Based on an analysis of the I-N and N-C coexistence concentrations, we observe that the ''effective physical'' aspect ratio in their case appears to be slightly lower as well, i.e., $L/D=1/17$.

A possible reason for the discrepancy between theory and experiment could lie in the shape characteristics of the particles. The experimental platelets are polydisperse hexagonal particles, while the model is based on monodisperse circular disks. Recently, Bates[23] has reported on the influence of particle shape of infinitely thin platelets on the I-N transition. It is found that the transition densities are lowered just by 10% when going from circular to hexagonal platelets. In a study of the influence of polydispersity on the I-N phase transition for infinitely thin hard platelets, Bates and Frenkel[24] find that the transition densities for 22%-polydisperse disks deviate more substantially from the monodisperse values ($c_I=3.56$ and $c_N=4.75$ versus 3.68, respectively, 3.98 for the monodisperse case). This leads us to the conclusion that the calculated individual phase heights could very well be influenced by particle shape and polydispersity, although it is unclear to what extent. To address this issue would require an equation of state and the chemical potentials[6] for a system of polydisperse hexagonal platelets.

V. CONCLUSION

We have studied the influence of gravity on a suspension of sterically stabilized colloidal gibbsite platelets (hard platelets). An initially I-N biphasic sample developed a columnar phase on the bottom of the sample by sedimentation of the particles. This dynamical sedimentation-diffusion equilibrium was reached on a time scale of a year. In order to describe the phenomenon, we used a simple osmotic compression model, requiring an equation of state for the platelets. These were obtained from literature and from Monte Carlo computer simulations that we performed. We find that the model describes the observed three-phase equilibrium quite well, be it for an aspect ratio that is significantly smaller than the experimental value.

ACKNOWLEDGMENTS

T.S. thanks Ronald Blaak for the algorithm to detect overlaps of cut spheres and NWO and Stichting FOM for access to the AMOLF computer cluster. H.L. thanks Jeroen van Duijneveldt for several insightful discussions on the hard-platelet equation of state.

[1] J. Perrin, Ann. Chim. Phys. **18**, 5 (1909).
[2] J. Perrin, *Les Atomes* (Libr. Felix Alcan, Paris, 1920).
[3] R. C. Williams, Proc. Natl. Acad. Sci. U.S.A. **70**, 1506 (1973).
[4] P. D. Ross and A. P. Minton, J. Mol. Biol. **112**, 437 (1977).
[5] R. Briehl and S. Ewert, J. Mol. Biol. **80**, 445 (1977).
[6] A. Vrij, J. Chem. Phys. **72**, 3735 (1980).
[7] R. S. Crandall and R. Williams, Science **198**, 293 (1977).
[8] K. Takano and S. Hachisu, J. Chem. Phys. **67**, 2604 (1977).
[9] B. J. Alder, W. G. Hoover, and D. A. Young, J. Chem. Phys. **49**, 3688 (1968).
[10] S. Hachisu and K. Takano, Adv. Colloid Interface Sci. **16**, 233 (1982).
[11] R. Piazza, T. Bellini, and V. Degiorgio, Phys. Rev. Lett. **71**, 4267 (1993).
[12] M. A. Rutgers, J. H. Dunsmuir, J.-Z. Xue, W. B. Russel, and P. M. Chaikin, Phys. Rev. B **53**, 5043 (1996).
[13] T. Biben, J. P. Hansen, and J. L. Barrat, J. Chem. Phys. **98**, 7330 (1993).
[14] G. Oster, J. Gen. Physiol. **33**, 445 (1950).
[15] U. Kreibig and C. Wetter, Z. Naturforsch. **35C**, 750 (1980).
[16] A. A. Brian, H. L. Frisch, and L. S. Lerman, Biopolymers **20**, 1305 (1981).
[17] F. M. van der Kooij and H. N. W. Lekkerkerker, J. Phys. Chem. B **102**, 7829 (1998).
[18] J. A. C. Veerman and D. Frenkel, Phys. Rev. A **45**, 5632 (1992).
[19] S.-D. Zhang, P. A. Reynolds, and J. S. van Duijneveldt, J. Chem. Phys. **117**, 9947 (2002).
[20] F. M. van der Kooij, K. Kassapidou, and H. N. W. Lekkerkerker, Nature (London) **406**, 868 (2000).
[21] D. van der Beek and H. N. W. Lekkerkerker, Langmuir (to be published).
[22] H. H. Wensink and H. N. W. Lekkerkerker, Europhys. Lett. **66**, 125 (2004).
[23] M. A. Bates, J. Chem. Phys. **111**, 1732 (1999).
[24] M. A. Bates and D. Frenkel, J. Chem. Phys. **110**, 6553 (1999).